CSIRO PUBLISHING
Australasian Plant Pathology, 2009, **38**, 110–119 www.publish.csiro.au/journals/app

Use of high resolution digital multi-spectral imagery to assess the distribution of disease caused by *Phytophthora cinnamomi* on heathland at Anglesea, Victoria

R. J. Hill[A,B], *B. A. Wilson*[A,C], *J. E. Rookes*[A] *and D. M. Cahill*[A,D]

[A]School of Life and Environmental Sciences, Deakin University, Geelong Campus at Waurn Ponds, Geelong, Vic. 3217, Australia.
[B]Present address: Ecoplan, Portland, Vic. 3305, Australia.
[C]Present address: Department of Environment and Conservation, Wanneroo, WA 6065, Australia.
[D]Corresponding author. Email: david.cahill@deakin.edu.au

Abstract. Disease caused by the soilborne plant pathogen *Phytophthora cinnamomi* causes long-term floristic and structural changes in native vegetation communities in Australia. Key components of the management of this disease are to know where it occurs and the rate at which it spreads. The distribution of *P. cinnamomi* has generally been assessed as locality points of infestation and mapping the extent of diseased vegetation in any area is difficult and costly. This study was undertaken in *P. cinnamomi*-infested heathland communities in southern Victoria, Australia, where the symptoms of *P. cinnamomi* arise as a mosaic within healthy vegetation. We investigated the potential to improve the efficiency and effectiveness of mapping and monitoring vegetation affected by *P. cinnamomi* using digital multi-spectral imaging. This technique was developed for the purposes of monitoring vegetation and provides a single, seamless ortho-rectified digital image over the total area of interest. It is used to spatially quantify small differences in the characteristics of vegetation. In this study, the symptoms of disease caused by *P. cinnamomi* infestation were related to differences in the imagery and were used to map areas of infestation. Comparison of the digital multi-spectral imaging indications with on-ground observations gave moderate accuracy between the datasets ($\kappa = 0.49$) for disease and healthy indications. This study demonstrates the ability of the technique to determine disease extent over broad areas in native vegetation and provides a non-invasive, cost effective tool for management.

Additional keywords: videography, *Xanthorrhoea*.

Introduction

The oomycete *Phytophthora cinnamomi* is a soilborne plant pathogen that causes widespread disease of native vegetation in Australia (Cahill *et al*. 2008). The symptoms of the disease include root and collar lesions, leaf chlorosis, retarded growth and death of plants. The pathogen primarily infects the roots of host plants causing root and collar rot that leads to a reduction in transpiration and nutrient uptake (Dawson and Weste 1984; Marks and Smith 1991; Cahill 1998). It has a wide host range, although its effects on individual species varies (Weste and Marks 1987). The disease can significantly alter both the floristic and structural composition of vegetation communities (Weste 2003). *P. cinnamomi* causes disease in a range of vegetation types including the jarrah (*Eucalyptus marginata*) forests of Western Australia, stringybark (*E. obliqua*) and silvertop ash (*E. sieberi*) forests of Victoria, and has been recorded in tropical rainforest of Queensland (Gadek 1998). It also occurs widely in species-rich woodland and heathland communities (Cahill *et al*. 2008).

Disease in natural systems caused by *P. cinnamomi* is listed as a key threatening process in Australia under the Commonwealth Environment Protection and Biodiversity Conservation Act 1999. The National Threat Abatement Plan for the disease caused by *P. cinnamomi* was developed (Environment Australia 2001) with major objectives to promote the recovery of threatened species and ecological communities under threat and to limit the spread of the pathogen into areas where it may lead to further species or communities becoming threatened. Recent national projects to address these objectives have developed processes and criteria to assess the risk to biodiversity from disease (Wilson *et al*. 2005) and national best practice benchmarks for management have been established (O'Gara *et al*. 2005). Key components for risk assessment and management of disease are: (1) to know where the disease occurs, (2) which species and communities are threatened, and (3) what the risks and consequences of infestation are. Mapping has usually been based on the presence or absence of susceptible species and on the presence of dead and dying plants. Due to the

 10.1071/AP08092 0815-3191/09/020110

widespread occurrence of *P. cinnamomi* in Australia detailed mapping of disease distribution has only been undertaken to a limited extent, for example, in Western Australia where relatively large areas of the affected jarrah forest have been comprehensively mapped (O'Gara *et al*. 2005).

In southern Victoria's Great Otway National Park, symptoms of disease were first identified in 1972 and have been continually observed throughout the area (Wark *et al*. 1987; Aberton *et al*. 2001; Wilson *et al*. 2003). Significant differences have been found in the floristics and structure between diseased and non-diseased vegetation (Laidlaw 1997), and infection of native vegetation is associated with low species richness and low abundance of small mammals (Wilson *et al*. 1994; Laidlaw 1997). In general terms in the Eastern Otways species from the families Proteaceae and Ericaceae and, especially the keystone monocotyledon *Xanthorrhoea australis*, are lost locally after infection and are replaced by sedges and rushes. Typically, at the boundary between diseased and non-diseased vegetation individual plants of susceptible species show disease symptoms and for a short distance behind the disease front dead individuals remain. However, symptoms may also be expressed as a mosaic among healthy vegetation.

Monitoring and measuring disease of plants, whether in the large-scale plant production systems of plantation forestry and agriculture or in biodiverse natural systems, is challenging. A variety of approaches have been used with a major goal of producing a disease incidence map that allows some sort of management decision to be made whether it is for disease control, eradication or maintenance of biodiversity or a combination of these (Ristaino and Gumpertz 2000; Stone *et al*. 2001; Holdenrieder *et al*. 2004). Mapping the total extent of disease caused by *P. cinnamomi* in Australia is considered to be a difficult goal to achieve. It may be impractical and for severely degraded sites, may not necessarily be warranted. For a pathogen such as *P. cinnamomi* that may progress quickly through the landscape, maps of distribution can become outdated and potentially misleading within a relatively short period of time.

Methods for mapping the extent of disease caused by *P. cinnamomi* have included on-ground surveys, interpretation of aerial photographs and aerial survey of symptoms using key indicator species (Hogg and Weste 1975; Cahill *et al*. 2002; Bluett *et al*. 2003; O'Gara *et al*. 2005). Limitations to such methods include cost, a lack of trained interpreters and insufficient spatial resolution of resultant maps for the required fine-scale management decisions. To overcome these difficulties for broad-scale disease mapping and assessment, remote sensing and image analysis have been widely tested and often adopted as tools for management (Nilsson 1995; Ristaino and Gumpertz 2000; Metternicht 2007; Olsson *et al*. 2008). Analysis and management of large crop or forestry areas and of native vegetation has increasingly used remote sensing techniques; for example, for estimations of forest biomass (Lucas *et al*. 2008), assessment of biodiversity (Turner *et al*. 2003; Gillieson *et al*. 2006) and habitat complexity (Coops and Catling 1997; Catling and Coops 2004), forest health (Chaerle and Van der Straeten 2000; Stone *et al*. 2001; Liu *et al*. 2006) and extent of crop disease (Zhang *et al*. 2003; Apan *et al*. 2004; Mirik *et al*. 2006; Lenthe *et al*. 2007). Remote sensing via airborne videography has emerged as an alternative to satellite imagery (see for example Lamb 2000) and is a rapid, non-invasive, cost effective method of providing geo-referenced maps at high spatial resolution for vegetation mapping and crop assessment. Here we examined airborne videography in combination with digital multi-spectral imaging as a tool to assess distribution of disease caused by *P. cinnamomi* in native vegetation – to our knowledge this is the first time this type of assessment on *P. cinnamomi* has taken place.

Methods

Study area

The study area was located 100 km south-west of Melbourne in the eastern Otway Ranges, Great Otway National Park, Victoria, Australia (Fig. 1*a*). It is public land within an area leased by Alcoa of Australia for brown coal extraction. The area, now known as the Anglesea Heath, covers an area of 6731 ha and is recognised for its significant flora and fauna communities and is co-managed by Alcoa and Parks Victoria (McMahon and Brighton 2002). The Anglesea Heath occurs on a dissected plateau, consisting of mainly Tertiary sediments overlying older Cretaceous strata (Abele 1971) and is drained by the Anglesea River. The soils are highly leached acidic podsol with a relatively loamy surface texture and acidic peat (Walbran 1971). The study was restricted to Bald Hills Heath (Land Conservation Council 1985; Meredith 1986; Wark *et al*. 1987) (vegetation type H3a, Meredith 1986). This vegetation type is a low heath that contains many species that are susceptible to *P. cinnamomi*.

For the purposes of this investigation the study area was delineated to include the main body of heath, an area of ~840 ha (Fig. 1*b*). The heath occupies a dissected plateau and is bound by taller vegetation. The roads and tracks, which traverse the area, were probably the source of the original infestation of *P. cinnamomi* (Wilson *et al*. 2003). The area has been subjected to wildfire in 1983 and controlled fuel reduction burning during the period 1991–93. Fire history and vegetation type were derived from existing maps (Vicmap, Department of Sustainability and Environment, East Melbourne, Vic., http://www.vicmap.com.au, verified 7 December 2008).

Field measurements and aerial digital imagery

The method that we used had two components. First, site data were collected in the form of visual interpretation of the symptoms of disease caused by *P. cinnamomi*. Second, the area was flown by light aircraft and remote, digital multi-spectral images (DMSI) were acquired for the site.

Field measurements

The field data were geo-referenced with an accuracy of 1 m using a differential global positioning system (DGPS, Leica Geosystems GS5PLUS , Heerbrugg, Switzerland) attached to a handheld computer, using ArcPad software (ESRI 2000). Field points (one DGPS point) were located by traversing the study area and selecting sites across the topography and representative of the full range of observed variation in the vegetation (descriptions and images of the heath and symptoms of disease have been described by Cahill *et al*. 2008). Each point was considered the centre of a circular plot 2 m in diameter and classified as healthy (species susceptible to *P. cinnamomi* present,

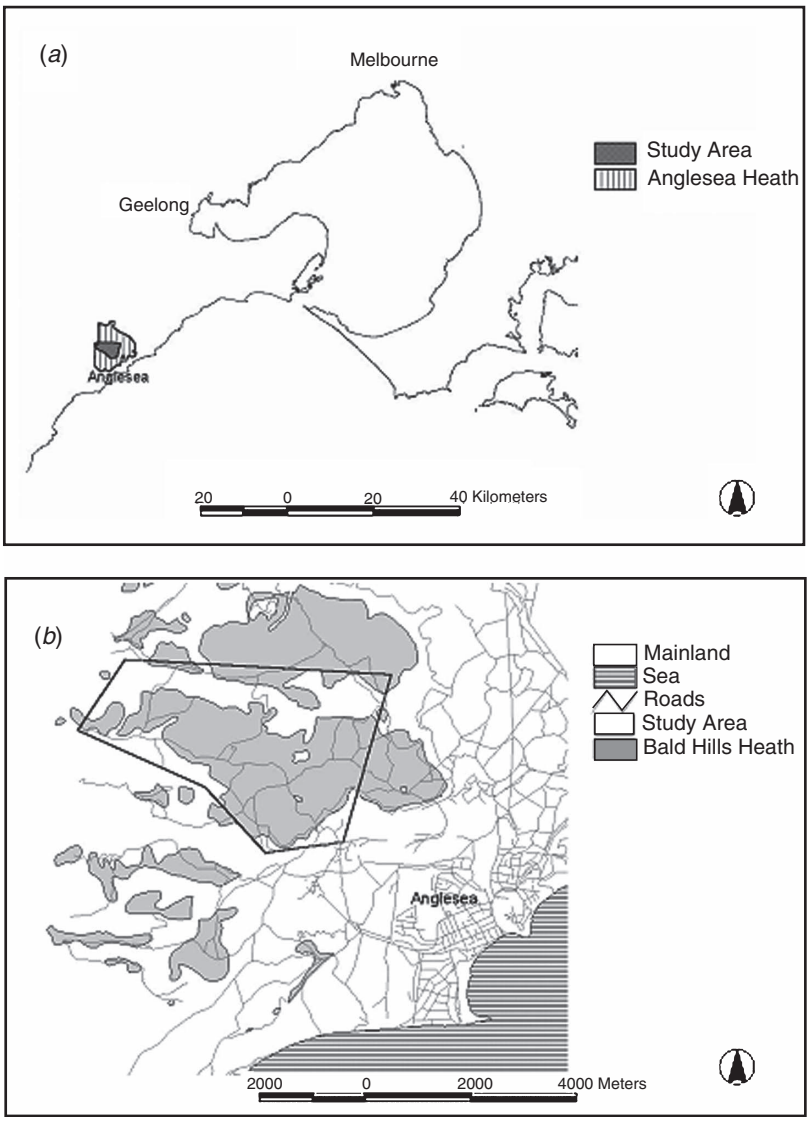

Fig. 1. (*a*) Locality plan showing the study area and the Anglesea Heath in relation to Anglesea, Geelong and Melbourne. (*b*) Locality plan showing the distribution of Bald Hills Heath within the study area.

especially *X. australis* of healthy appearance), or diseased (susceptible species present but dying or dead). Previous studies within the study area had confirmed the presence of *P. cinnamomi* by soil baiting and its association with symptom production, plant decline and death (Laidlaw 1997; Laidlaw and Wilson 2003; Wilson *et al*. 2003). In determining point locations various aspects and situations within the topography of the heath were sampled. A total of 63 points were plotted (Fig. 2). Furthermore, we used a site that had been mapped as healthy patches within generally diseased vegetation in 1999 using GPS (W. S. Laidlaw, pers. comm.) to check our DMSI classifications.

Collection and extraction of data from aerial imagery

SpecTerra Services (Leederville, Western Australia) has developed DMSI and provide image acquisition and processing services for the purposes of vegetation monitoring. The imagery is gathered in four wavebands, 25 nm wide, centred about the principal reflectance features of vegetation in the blue, green, red and near infrared portions of the spectrum (Table 1). In July 2002, the Anglesea heathlands were flown by SpecTerra and DMSI was provided in a 2 by 2-m cell or pixel size.

DMSI is pre-processed to correct for camera distortions and bi-directional reflectance (variation in brightness across an image due to changing angle and intensity of reflected sunlight). It is provided as a seamless ortho-rectified digital image, which can be displayed in a geographic information system (GIS) as natural colour or false colour infrared images. Because the image is taken using videography and is seamless it may cover a large area. Any relationship developed between imagery and ground variation remains constant over the

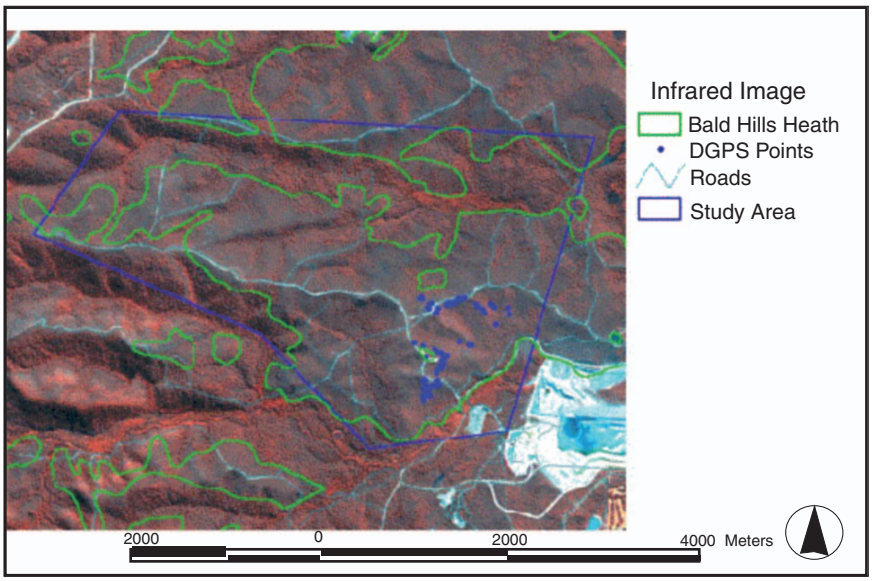

Fig. 2. Infrared image of the study area showing Bald Hills Heath and the differential global positioning system point locations. The topography and relative elevation of landscape units within the study area can be distinguished as can geographical features such as ridges, gullies and streamlines. Several roads traverse the site and can be seen as white to off-white lines though the landscape, especially in association with high ground such as ridgelines. The industrial area to the south-east of the study site is an Alcoa of Australia open-cut coal mine.

Table 1. Wavelength bands used for digital multi-spectral imagery

Spectral band	Blue	Green	Red	Infrared
Wavelength (nm)	438–462	538–562	638–762	758–782

whole image. The infrared image of the study area is shown in Fig. 2. Images of the same area taken at different times (but with similar solar angle) are directly comparable.

Data were extracted from the imagery within the GIS using the ArcView Image Analysis extension; spectral categorisation used an unsupervised approach (ISODATA algorithm, ERDAS 2000). This system enabled tasks that ranged from simply displaying images to performing detailed spectral analysis. Image classification and image analysis were important aspects of this study: (1) image classification was based on the spectral values of the data the imagery contains and was used to group the data into vegetation classes, and (2) image analysis was used to determine plant pigment ratio, plant vigour ratio and plant cell density ratio (Kaufman and Tanre 1992; Metternicht 2007).

Further, categorisation was based on spectral values using an iterative, self-organising data analysis technique linked with a convergence threshold. This technique categorised single or multi-band continuous data to create thematic or categorised data. Each cell of the imagery had four digital numbers (DN) that correspond with the values of the four spectral bands at that point. The statistics are re-calculated, on each iteration, as cell similarity is evaluated. The process was repeated until at least 95% of cells remain in the same class between iterations. The effect is to reinforce any patterns in the data by displaying like with like and enhancing differences. The number of classes is selected for each application to optimise the pattern discrimination; patterns appear weaker if the number is either too low or too high. For this study 12 classes were chosen.

Analysis was based on normalised difference ratio images (NDRI) prepared from the DMSI by dividing the difference in DN between two bands with the sum of the DN for the bands on a pixel-by-pixel basis, that is NDRI = (DN1 – DN2)/(DN1 + DN2). This is said to 'normalise' the data because it reduces the effect of surface slope, (which affects the amount of light reflected) and overall illumination. Three NDRI were prepared from the data as follows:

Plant pigment ratio (PPR)

PPR was prepared with the green band (Table 1) as DN1 (not strongly absorbed and is essentially reflected by any components of vegetation, acts as a 'reference') and the blue band as DN2 (absorbed strongly by plant pigments such as chlorophylls and carotenoids). PPR is higher for more pigmented vegetation.

Plant vigour ratio (PVR)

PVR was prepared with green as DN1 and red as DN2 (absorbed by chlorophyll). The ratio is higher where plants are actively photosynthesising, and, therefore, strongly absorb in the red band and reflect light in the green band. Lower PVR represents less photosynthetically active vegetation that may be a consequence of stress, nutrient deficiencies or disease.

Plant cell density ratio (PCD)

This parameter is equivalent to the normalised difference vegetation index used by Kaufman and Tanre (1992). The

index is a measure of red light absorption by chlorophyll cf. that reflected in the near infrared. PCD is higher where vegetation is in good health or has high biomass (Metternicht 2007). PCD was prepared with infrared as DN1 and red as DN2.

These ratios were combined in a false colour composite image by allocating PCD to red, PVR to green and PPR to blue to highlight and reinforce any patterns in the data. Field data were compared with image data (the three ratios and the composite image) using the coordinates of the field points. A critical aspect of this method was the establishment of a close relationship between image class and on-ground variations in vegetation, which depended substantially on the number of image classes used. If the number was too high extraneous divisions were identified in the vegetation (for example a vegetation type may separate into two image classes based on the light and shady side of the plant). If the number was too low real differences in the vegetation were lost. The appropriate number of image classes depends on the scale of the photography and the vegetation type and can only be determined by experimentation and field checking.

Results

The study area has been the subject of several previous studies and *P. cinnamomi* has been frequently isolated from soil and roots of symptomatic vegetation within the study area boundaries (for example Laidlaw 1997; Laidlaw and Wilson 2003; Wilson *et al*. 2003). The infrared image (Fig. 2) showed variations in the intensity of red colouration indicating variations in vegetation type and cover across the study site. A higher intensity of redness was observed for vegetation in lower lying, south-facing areas and in association with gullies and streamlines. A lower intensity of redness occurred at higher elevations, on north facing slopes and in association with heath vegetation. The DGPS point locations are also shown in Fig. 2. The unsupervised classification defined 12 distinct categories (Fig. 3). Note that the composite rather than ratio image is used here and in subsequent examples, because the patterns were less defined in the ratio images (data not shown). The images were sampled using the coordinates of the field DGPS points and the number of cells in each class was determined. The percentage of cells in each class for points on diseased and on healthy vegetation is shown in Fig. 4*a*. The percentage area for each class varied within both diseased and healthy vegetation and between the two. To determine the classes that were potentially useful for differentiating between diseased and healthy vegetation, for each category the area for healthy was subtracted from the area for diseased (Fig. 4*b*). Each category could then be evaluated on the basis of the largest differences in the percentage areas within each image class between healthy and diseased vegetation. The largest increases in area associated with the transition from healthy to diseased vegetation occurred in image classes 1 and 5 (13 and 9%, respectively), while the largest decreases in area within image classes that were associated with the transition from healthy to diseased vegetation occurred in image classes 4, 8 and 10 (7, 13 and 15%, respectively). Where the difference in percentage area occupied by an image class between healthy and diseased vegetation was less than 5 percent, the difference was judged to be not material and these categories were considered to indicate no change in status.

It was postulated that an increase in the percentage area of a particular image class within diseased vegetation was associated with the particular combination of vegetation found during or after infection (e.g. rushes and sedges) and designated as *P. cinnamomi* affected. The opposite effect (an increase in the percentage in the healthy zone was associated with the vegetation growing in the absence of disease (e.g. species from the families Proteaceae and Xanthorrhoeacea) and designated healthy. This interpretation was evaluated by comparing the overall distribution of

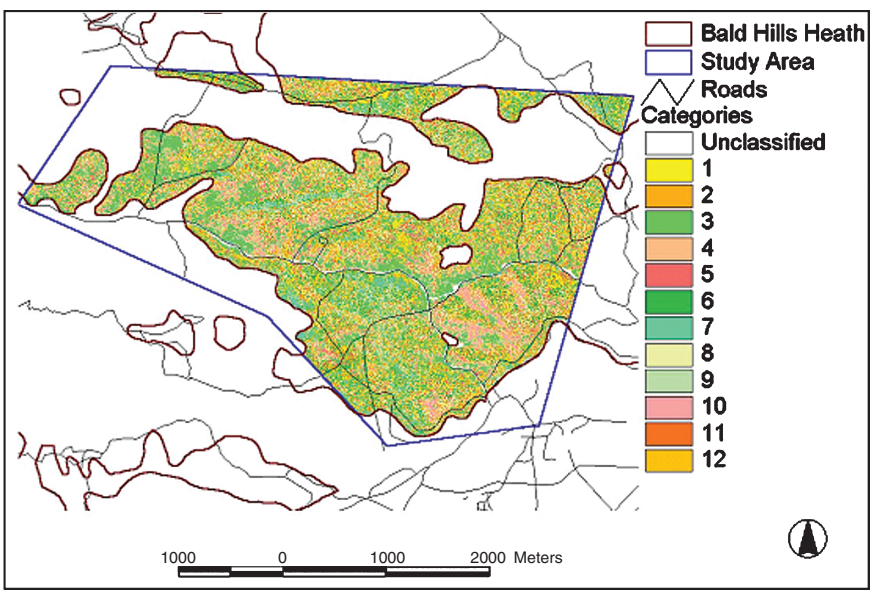

Fig. 3. Composite image of the Bald Hills study area showing the distribution of 12 image classes.

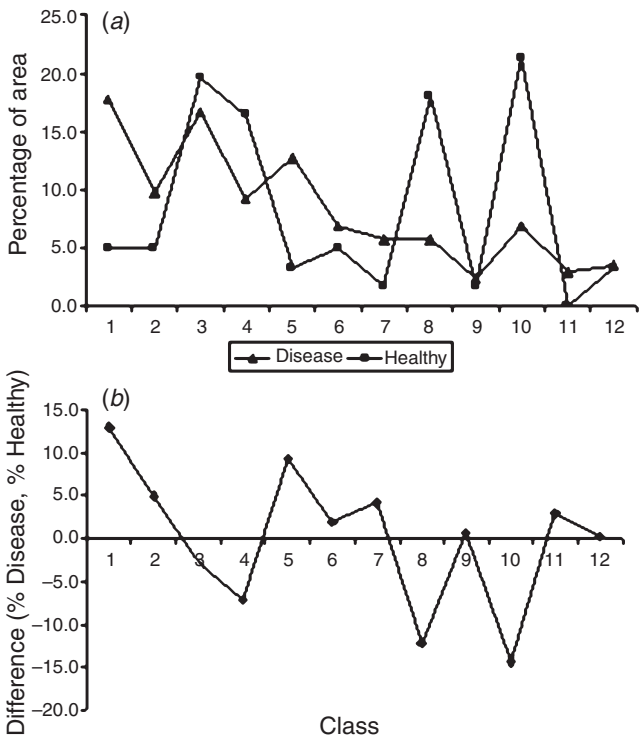

Fig. 4. (*a*) Percentage of Bald Hills Heath in each of the 12 image classes for diseased and healthy vegetation. (*b*) Differences in the percentage of area of the Bald Hills Heath in each of 12 image classes between diseased and healthy vegetation.

affected and healthy indications with known vegetation condition from the field sites. For visual convenience, pixels in Fig. 5 that represent indications of a *P. cinnamomi* effect were coloured red, pixels representing the healthy indications were coloured green, and the remaining pixels were coloured grey (where the percentage area change was less than 5%).

Applying a smooth filter to the data for the northern group of DGPS sites reduced background speckle in the digitised images. Smoothing applied a convolution kernel throughout the image to provide the most common class value within a 3-by-3 matrix to the target pixel and reduced the number of small areas derived from a categorisation. A simple visual comparison of the smoothed image (Fig. 6) shows that the pixel-by-pixel indication of vegetation status and the measured state on the ground corresponds. A statistical measure of the degree of correspondence, beyond chance, is the kappa coefficient (Kadmon *et al*. 2004; Wagner *et al*. 2008). When DGPS sites in healthy and disease indications in Fig. 6 were compared (excluding those lying in the neutral classification) with that of the on-ground state there was a moderate level of correlation ($\kappa = 0.49$). However, if DGPS sites in close proximity to expected indications are accepted (including those in the neutral indication), there was stronger agreement between datasets ($\kappa = 0.84$).

The relationship between visual indication of disease status and the measured state on the ground was further tested at a plot (see Fig. 5 for location) that had been established 3 years earlier in an area of complex disease spread (W. S. Laidlaw, pers. comm.). The healthy patches, where *P. cinnamomi* had not been isolated and where there were no symptoms of disease, were previously designated by GPS waypoints and are shown in Fig. 7. The DMSI indicated that the healthy patches now contained some areas of disease. These patches were ground-truthed, following capture of the DMSI data, for presence of disease symptoms. Visual observations confirmed that there were now symptoms of disease in corresponding areas within the patches.

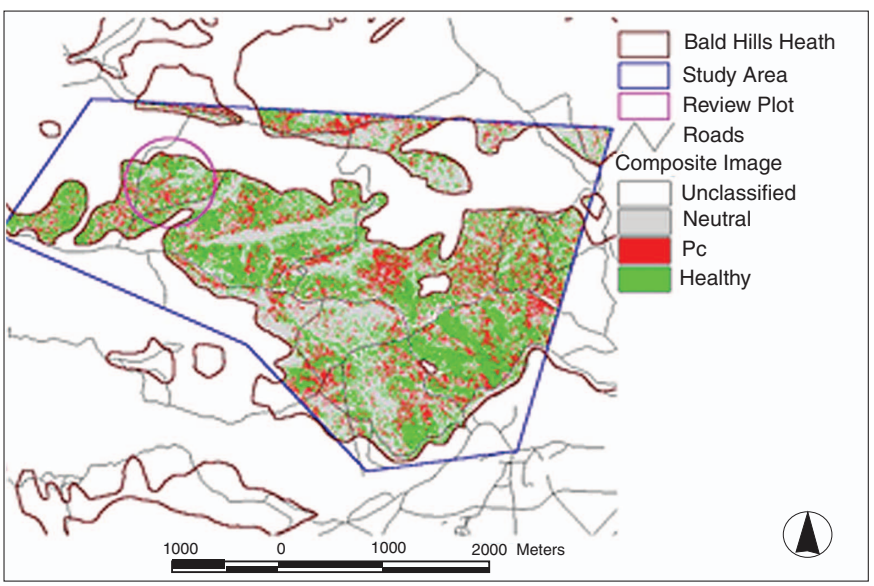

Fig. 5. Distribution of 2 by 2-m pixels in the Bald Hills Heath showing image classes that decrease in area by 5 percent or more (healthy indications, 'Healthy') or increase in area by 5 percent or more (disease indications, 'Pc') between diseased and healthy vegetation.

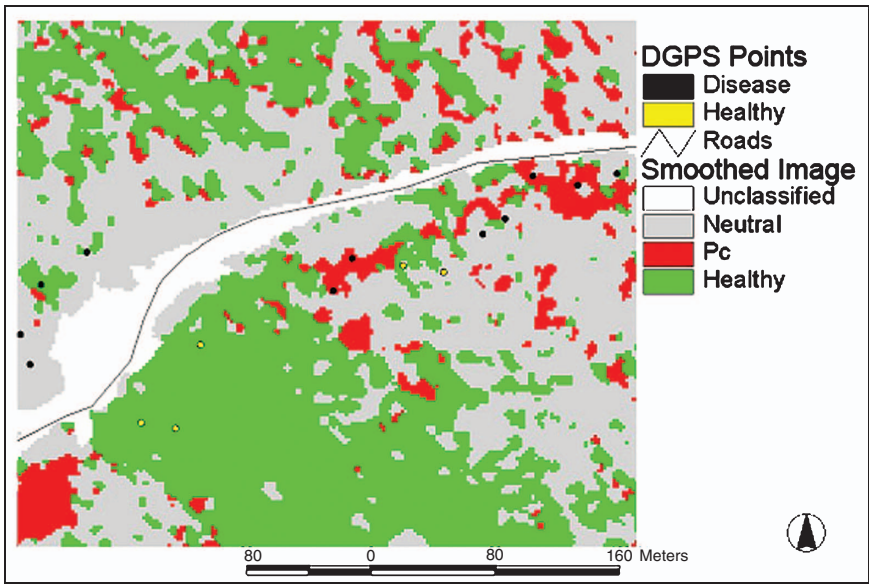

Fig. 6. Smoothed image showing distribution of pixels in a portion of the Bald Hills Heath showing a decrease in area by 5 percent or more (healthy indications) or increase in area by 5 percent or more (disease indications) between diseased and healthy vegetation. Note that the 'unclassified area' designation shows areas that have been completely cleared of vegetation (road easement and a gravel pit).

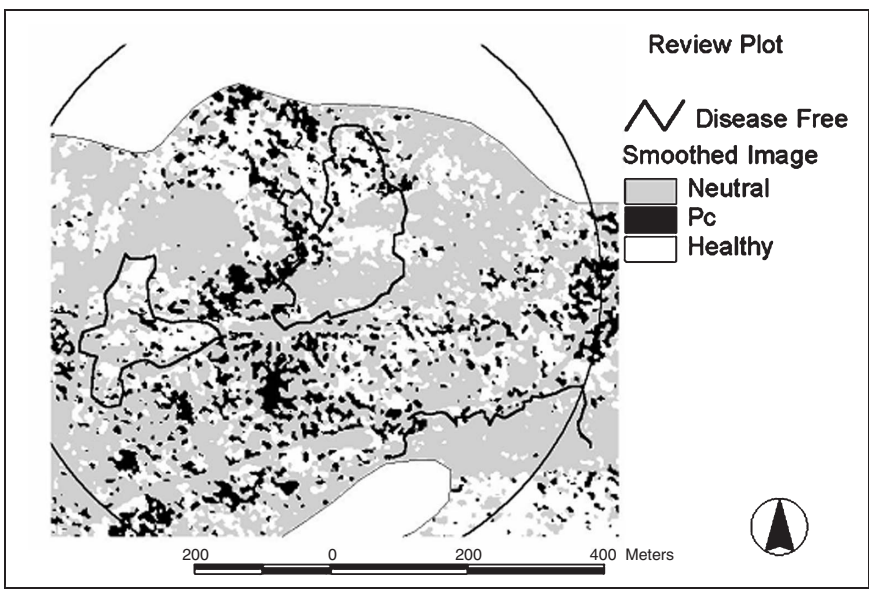

Fig. 7. Detail of disease indication at a review plot in the western part of the study area. The two shapes centrally within the review plot delineate areas that were mapped in 1999 and were designated as free of disease symptoms. In this image vegetation that shows disease indication is black while a healthy indication is designated as white.

The data compiled can be used to determine relative extent across the study site of vegetation that shows disease compared with that which is healthy or neutral. Table 2 provides a simple quantification of disease provided it is recognised that the actual disease cover is likely to be greater; at least some of the neutral area may represent sites where disease has passed through and where symptoms of disease may no longer be present but there has been vegetation change.

Table 2. Area and percentage of Bald Hills Heath within the study area in each class of disease indication

Disease indication	Area (ha)	Percentage of heath
Diseased	154.8	18.43
Healthy	217	25.84
Neutral	468	55.73
Total	839.8	100.00

Discussion

We have spatially examined differences in vegetation appearance using DMSI to provide fine-scale information of the distribution of disease caused by *P. cinnamomi* on a susceptible heathland vegetation community. We propose that the fine detail in the DMSI data could be used to determine the presence and position of disease fronts and broader areas of infestation within heathland and open forest communities at much finer scale than is possible with other methods. Correlation between the disease status derived from DMSI and the observed and measured state on the ground showed a moderate to high level of agreement depending on the stringency of comparison. Further, regular application of DMSI at the resolution used, or greater (for example, 25-cm pixel size, Hall *et al*. 2003; Metternicht 2007), could permit direct pixel-by-pixel comparison and enable change mapping and estimates of disease progression at the detail of individual plants lost to disease. Feedback at this level would enable fine-tuning and precise evaluation of control strategies.

Our analysis using DMSI was extended to a review plot that had been previously assessed for disease status. The DMSI designation of the disease status of vegetation and the field delineation of disease-free patches in the review plot showed similar distributions of disease. The delineations of symptomatic and asymptomatic vegetation were reasonably well defined by the waypoints derived from non-differential GPS given the positioning error may have been as high as 10 m. The disease class in the DMSI indication does, however, show that areas of the review plots that were deemed to be healthy may now not be entirely free of disease and this was confirmed by ground truthing.

The DMSI maps showed the disease indication to be concentrated in particular areas and along roads (patterns expected for disease spread) and it was also lightly spread over much of the remaining area. This pattern indicates that across the study area some vegetation showed the typical symptoms associated with disease presence. Similarly, there was some healthy indication within concentrated disease areas. This may be explained by: (1) the absoluteness of rating every cell (2 by 2 m) as neutral or indicative of disease or health is not supported by the data; for example, an image class highly indicative of a particular disease status may occur with the opposite disease status and in the output map appears as a speckle of contra indication even in areas where the disease status is strongly indicated, (2) the presence of inliers of healthy vegetation (perhaps 'disease escapes') and individually field-resistant plants within generally diseased areas and, (3) vegetation such as sedges and rushes that occur naturally without disease association. However, the overall effect of background speckle has little practical significance and may be safely ignored in most circumstances. It is analogous to the rationalisation inherent in determining broad area disease status using current on-ground techniques where individual plants are not considered when disease fronts are drawn.

This work was based on the premise that the study area where the DGPS points were set essentially consisted of one vegetation type and this may not have been true, for example, the neutral indication was concentrated in bands. Further inspection of these areas showed them to be the upper northerly (drier) aspect of the low ridges that traverse the study area and that the vegetation was lower and more open than the normal Bald Hills Heath (whether diseased or not). The vegetation was typical of that altered by the passage of disease (Cahill *et al*. 2008) and where the disease is found in association with roads and tracks, susceptible species in adjoining vegetation are killed and a less complex, post-disease community comprising sedges and grasses remains. Thus, the neutral indication may be useful for designation of previously infested sites.

The use of DMSI to spatially quantify small differences in vegetation appearance across large areas and relate this to vegetation condition has important management as well as monitoring applications. This study was limited to evaluating disease spread in portions of what was thought to be one vegetation type within the Anglesea Heath (840 ha in over 6500 ha). The remaining, more remote, areas of Bald Hills Heath can now be evaluated using the same relationships and imagery, and with relatively few extra field plots all the heath and open heathy woodland could also be assessed. A study of this magnitude could not be achieved using current methods without very intensive ground survey.

In conclusion, a system for assessing *P. cinnamomi*-related disease in the Bald Hills Heath in southern Victoria has been demonstrated using DMSI. Fine detail maps were produced which gave a more complete picture and were easier to interpret than the results of current methods that use aerial photography and interpolation between limited numbers of ground-based monitoring sites. This system is well founded and simple. Change mapping between successive monitoring periods was not demonstrated but would be simple and could be used to show if the vegetation is declining, static or recovering. The data could also be used with current predictive mapping algorithms (Wilson *et al*. 2003; Bergot *et al*. 2004) especially under various climate change scenarios (Garrett *et al*. 2006; Kluza *et al*. 2007) and will be of great use in future attempts at control and for limiting the spread of the pathogen into uninfested sites.

Acknowledgements

We thank Alcoa of Australia and, in particular, mine manager Chris Rolland for advice, and the Australian Research Council for financial support. JER was funded by the Australian Government Department of the Environment, Water, Heritage and the Arts.

References

Abele C (1971) 'Physiography, geology and mineral resources. Resources Survey Barwon Region.' (Government of Victoria: Melbourne)

Aberton MJ, Wilson BA, Hill J, Cahill DM (2001) Development of disease caused by *Phytophthora cinnamomi* in mature *Xanthorrhoea australis*. *Australian Journal of Botany* **49**, 209–219. doi: 10.1071/BT00065

Apan A, Held A, Phinn S, Markley J (2004) Detecting sugarcane 'orange rust' disease using EO-1 Hyperion hyperspectral imagery. *International Journal of Remote Sensing* **25**, 489–498. doi: 10.1080/01431160310001618031

Bergot M, Cloppet E, Perarnaud V, Deque M, Marcais B, Desprez-Loustau M-L (2004) Simulation of potential range expansion of oak disease caused by *Phytophthora cinnamomi* under climate change. *Global Change Biology* **10**, 1539–1552. doi: 10.1111/j.1365-2486.2004.00824.x

Bluett V, Weste G, Cahill D (2003) Distribution of disease caused by *Phytophthora cinnamomi* in Wilsons Promontory National Park and potential for further impact. *Australasian Plant Pathology* **32**, 479–491. doi: 10.1071/AP03048

Cahill DM (1998) General biology and ecology of *Phytophthora* with special reference to *Phytophthora cinnamomi*. In 'Patch deaths in tropical Queensland forests: association and impact of *Phytophthora cinnamomi* and other soilborne pathogens'. (Ed. PA Gadek) pp. 21–26. (CRC for Tropical Rainforest Ecology: Cairns)

Cahill DM, Harding C, O'May J, Wilson BA (2002) Assessment of guidelines for best practice management of *Phytophthora cinnamomi* in parks and reserves across Victoria. Report for Parks Victoria, University of Ballarat, Victoria.

Cahill DM, Rookes JE, Wilson BA, Gibson L, McDougall KL (2008) *Phytophthora cinnamomi* and Australia's biodiversity: impacts, predictions and progress towards control. *Australian Journal of Botany* **56**, 279–310. doi: 10.1071/BT07159

Catling P, Coops N (2004) Identification of species and functional groups that give early warning of major environmental change (indicator 1.2c). Part B: report on the efficacy of videography (and other high spatial resolution imagery) for habitat mapping. Report for the Forest and Wood Products Research and Development Corporation, Australian Government, Canberra. 13 pp.

Chaerle L, Van der Straeten D (2000) Imaging techniques and the early detection of plant stress. *Trends in Plant Science* **5**, 495–501. doi: 10.1016/S1360-1385(00)01781-7

Coops NC, Catling PC (1997) Using airborne multispectral videography to predict habitat complexity in eucalypt forest for wildlife management. *Wildlife Research* **24**, 691–703. doi: 10.1071/WR96099

Dawson P, Weste G (1984) Impact of root infection by *Phytophthora cinnamomi* on the water relations of two *Eucalyptus* species that differ in susceptibility. *Phytopathology* **74**, 486–490. doi: 10.1094/Phyto-74-486

Environment Australia (2001) 'Threat abatement plan for dieback caused by the root-rot fungus (*Phytophthora cinnamomi*).' (Environment Australia: Canberra)

ERDAS (2000) 'ArcView Image Analysis.' (ERDAS Inc.: Atlanta, GA) 256 pp.

ESRI (2000) 'Using ArcPad.' (Environmental Systems Research Institute Inc.: Redlands, CA) 70 pp.

Gadek PA (1998) 'Patch deaths in tropical Queensland forests: association and impact of *Phytophthora cinnamomi* and other soilborne pathogens.' (CRC for Tropical Rainforest Ecology: Cairns) 98 pp.

Garrett KA, Dendy SP, Frank EE, Rouse MN, Travers SE (2006) Climate change effects on plant disease: genomes to ecosystems. *Annual Review of Phytopathology* **44**, 489–509. doi: 10.1146/annurev.phyto.44.070505.143420

Gillieson DS, Lawson TJ, Searle L (2006) 'Applications of high resolution remote sensing in rainforest ecology and management.' (Cooperative Research Centre for Tropical Rainforest Ecology and Management. Rainforest CRC: Cairns) 54 pp.

Hall A, Louis J, Lamb D (2003) Characterising and mapping vineyard canopy using spatial-resolution aerial multispectral images. *Computers & Geosciences* **29**, 813–822. doi: 10.1016/S0098-3004(03)00082-7

Hogg J, Weste G (1975) Detection of die-back disease in the Brisbane Ranges by aerial photography. *Australian Journal of Botany* **23**, 775–781. doi: 10.1071/BT9750775

Holdenrieder O, Pautasso M, Weisberg PJ, Lonsdale D (2004) Tree disease and landscape processes: the challenge of landscape pathology. *Trends in Ecology & Evolution* **19**, 446–452. doi: 10.1016/j.tree.2004.06.003

Kadmon R, Farber O, Danin A (2004) Effect of roadside bias on the accuracy of predictive maps produced by bioclimatic models. *Ecological Applications* **14**, 401–413. doi: 10.1890/02-5364

Kaufman Y, Tanre D (1992) Atmospherically resistant vegetation index (ARVI) for EOS-MODIS. *IEEE Transactions on Geoscience and Remote Sensing* **21**, 245–273.

Kluza DA, Vieglais DA, Andreasen JK, Peterson AT (2007) Sudden Oak death: geographic risk estimates and predictions of origins. *Plant Pathology* **56**, 580–587. doi: 10.1111/j.1365-3059.2007.01602.x

Laidlaw WS (1997) The effects of *Phytophthora cinnamomi* on the flora and fauna of the Eastern Otways. PhD Thesis, Deakin University, Geelong.

Laidlaw WS, Wilson BA (2003) Floristic and structural changes of a coastal heathland exhibiting symptoms of *Phytophthora cinnamomi* infestation in the Eastern Otway Ranges, Victoria. *Australian Journal of Botany* **51**, 283–293. doi: 10.1071/BT02100

Lamb DW (2000) The use of qualitative airborne multispectral imaging for managing agricultural crops – a case study in south-eastern Australia. *Australian Journal of Experimental Agriculture* **40**, 725–738. doi: 10.1071/EA99086

Land Conservation Council (1985) Report on the Melbourne Area, District 1 – Review. Land Conservation Council, Melbourne.

Lenthe J-H, Oerke E-C, Dhene H-W (2007) Digital infrared thermography for monitoring canopy health of wheat. *Precision Agriculture* **8**, 15–26. doi: 10.1007/s11119-006-9025-6

Liu D, Kelly M, Gong P (2006) A spatial-temporal approach to monitoring forest disease spread using multi-temporal high spatial resolution imagery. *Remote Sensing of Environment* **101**, 167–180. doi: 10.1016/j.rse.2005.12.012

Lucas RM, Lee AC, Bunting PJ (2008) Retrieving forest biomass through integration of CASI and LiDAR data. *International Journal of Remote Sensing* **29**, 1553–1577. doi: 10.1080/01431160701736497

Marks GC, Smith IW (1991) The cinnamon fungus in Victorian forests. Lands and Forests Bulletin No. 31. Department of Conservation and Environment, East Melbourne.

McMahon K, Brighton M (2002) 'Anglesea Heath management plan November 2002.' (Parks Victoria and Alcoa World Alumina Australia Publishers: Melbourne) 56 pp.

Meredith C (1986) The vegetation of the Anglesea lease area. Report prepared for the Land Conservation Council, Government of Victoria, Melbourne.

Metternicht G (2007) Vegetation indices derived from high-resolution airborne videography for precision crop management. *International Journal of Remote Sensing* **24**, 2855–2877.

Mirik M, Michels GJ Jr, Kassymzhanova-Mirik S, Elliot NC, Catana V, Jones DB, Bowling R (2006) Using digital image analysis and spectral reflectance data to quantify damage by greenbug (Hemiptera: Aphididae) in winter wheat. *Computers and Electronics in Agriculture* **51**, 86–98. doi: 10.1016/j.compag.2005.11.004

Nilsson H-E (1995) Remote sensing and image analysis in plant pathology. *Annual Review of Phytopathology* **15**, 489–527. doi: 10.1146/annurev.py.33.090195.002421

O'Gara E, Howard K, Wilson B, Hardy GEStJ (2005) 'Management of *Phytophthora cinnamomi* for biodiversity conservation in Australia: Parts 1 & 2.' (Department of Environment and Heritage: Canberra)

Olsson H, Schneider W, Koukal T (2008) 3D remote sensing in forestry. *International Journal of Remote Sensing* **29**, 1239–1242. doi: 10.1080/01431160701736539

Ristaino JB, Gumpertz ML (2000) New frontiers in the study of dispersal and spatial analysis of epidemics caused by species in the genus *Phytophthora*. *Annual Review of Phytopathology* **38**, 541–576. doi: 10.1146/annurev.phyto.38.1.541

Stone C, Old K, Kile G, Coops N (2001) Forest health monitoring in Australia: national and regional commitments and operational realities. *Ecosystem Health* **7**, 48–58. doi: 10.1046/j.1526-0992.2001.007001048.x

Turner W, Spector S, Gardiner N, Fladeland M, Sterling E, Steininger M (2003) Remote sensing for biodiversity and conservation. *Trends in Ecology & Evolution* **18**, 306–314. doi: 10.1016/S0169-5347(03)00070-3

Wagner W, Hollaus M, Briese C, Ducic V (2008) 3D vegetation mapping using small-footprint full-waveform airborne laser scanners. *International Journal of Remote Sensing* **29**, 1433–1452. doi: 10.1080/01431160701736398

Walbran WI (1971) Soils. In 'Barwon Region Resources Survey'. pp. 52–218. (Central Planning Authority: Melbourne)

Wark MC, White MD, Robertson DJ, Marriott PF (1987) Regeneration of heath and heath woodland in the north-eastern Otway Ranges, Australia, following the wildfire of February 1983. *Proceedings of the Royal Society of Victoria* **99**, 51–88.

Weste GM (2003) The dieback cycle in Victorian forests: a 30-year study of changes caused by *Phytophthora cinnamomi* in Victorian open forests, woodlands and heathlands. *Australasian Plant Pathology* **32**, 247–256. doi: 10.1071/AP03013

Weste GM, Marks GC (1987) The biology of *Phytophthora cinnamomi* in Australian forests. *Annual Review of Phytopathology* **25**, 207–229. doi: 10.1146/annurev.py.25.090187.001231

Wilson BA, Newell G, Laidlaw WS, Friend G (1994) Impact of plant disease on faunal communities. *Journal of the Royal Society of Western Australia* **77**, 139–144.

Wilson BA, Lewis A, Aberton J (2003) Spatial model for predicting the presence of cinnamon fungus (*Phytophthora cinnamomi*) in sclerophyll vegetation communities in south-eastern Australia. *Austral Ecology* **28**, 108–115. doi: 10.1046/j.1442-9993.2003.01253.x

Wilson BA, Howard K, O'Gara E, Hardy GEStJ (2005) Management of *Phytophthora cinnamomi* for biodiversity conservation in Australia. Part 3 – Risk Assessment for Threats to Ecosystems, Species and Communities: a review. A report funded by the Commonwealth Government Department of the Environment and Heritage by the Centre for *Phytophthora* Science and Management, Murdoch University, Western Australia. 67 pp.

Zhang M, Qin Z, Liu X, Ustin SL (2003) Detection of stress in tomatoes induced by late blight disease in California, USA, using hyperspectral remote sensing. *International Journal of Applied Earth Observation and Geoinformation* **4**, 295–310. doi: 10.1016/S0303-2434(03)00008-4

Manuscript received 11 June 2008, accepted 23 October 2008